DIGITAL ACCESS TO SCHOLARSHIP AT HARVARD
DASH.HARVARD.EDU

HARVARD LIBRARY
Office for Scholarly Communication

Atomic Layer Deposition of Lanthanum-Based Ternary Oxides

Citation
Wang, Hongtao, Jun-Jieh Wang, Roy Gerald Gordon, Jean-Sébastien M. Lehn, Huazhi Li, Daewon Hong, and Deo V. Shenai. 2009. Atomic layer deposition of lanthanum-based ternary oxides. Electrochemical and Solid-State Letters 12(4): G13-G15.

Published Version
doi:10.1149/1.3074314

Permanent link
http://nrs.harvard.edu/urn-3:HUL.InstRepos:9310888

Terms of Use
This article was downloaded from Harvard University's DASH repository, and is made available under the terms and conditions applicable to Other Posted Material, as set forth at http://nrs.harvard.edu/urn-3:HUL.InstRepos:dash.current.terms-of-use#LAA

Share Your Story

The Harvard community has made this article openly available.
Please share how this access benefits you. Submit a story .

Accessibility

Electrochemical and Solid-State Letters, **12** (4) G13-G15 (2009)
1099-0062/2009/12(4)/G13/3/$23.00 © The Electrochemical Society

Atomic Layer Deposition of Lanthanum-Based Ternary Oxides

Hongtao Wang,[a] Jun-Jieh Wang,[b] Roy Gordon,[b,*,z] Jean-Sébastien M. Lehn,[c] Huazhi Li,[c] Daewon Hong,[c] and Deo V. Shenai[c]

[a]School of Applied Science and Engineering and [b]Department of Chemistry and Chemical Biology, Harvard University, Cambridge, Massachusetts 02138, USA
[c]Rohm and Haas Electronic Materials, North Andover, Massachusetts 01845, USA

Lanthanum-based ternary oxide $La_xM_{2-x}O_3$ (M = Sc, Lu, or Y) films were deposited on HF-last Si substrates by atomic layer deposition. Both $LaScO_3$ and $LaLuO_3$ films are amorphous while the as-deposited $La_xY_{2-x}O_3$ films form a polycrystalline layer/amorphous layer structure on Si. Transmission electron microscopy and electrical analysis show the absence of interfacial layers. The dielectric constants for $LaScO_3$, $LaLuO_3$, and $La_{1.23}Y_{0.77}O_3$ films are ~23, 28 ± 1, and 17 ± 1.3, respectively, with leakage current density up to 6 orders of magnitude lower than that of thermal SiO_2 with the same effective oxide thickness. Conformal coating thickness is demonstrated on holes with aspect ratio ~80:1.
© 2009 The Electrochemical Society. [DOI: 10.1149/1.3074314] All rights reserved.

Manuscript submitted November 30, 2008; revised manuscript received January 5, 2009. Published January 29, 2009.

Hafnium oxide has been widely studied as an alternative gate dielectric to replace silicon dioxide for metal-oxide-semiconductor field-effect transistors (MOSFETs) and dynamic random access memories. In 2007, Intel Corporation announced its accomplishment of integrating HfO_2 into MOSFETs with the physical gate length of 45 nm.[1] However, pure HfO_2 is readily crystallized at temperatures as low as ~500°C.[2] Amorphous dielectrics with high thermal stability are still preferred because they have no intrinsic defects, such as grain boundaries, and show homogeneous electrical properties, provided they still have the advantages of HfO_2, such as high dielectric constant ($\kappa \sim 22$ to 23), wide bandgap ($E_g = 5.5$ eV), and low leakage.[3] Recent reports show that lanthanum-based ternary oxides, such as lanthanum scandate ($LaScO_3$) and lanthanum lutetium oxide ($LaLuO_3$), can meet all these requirements. These materials were grown by molecular beam deposition,[4] pulsed laser deposition,[5] or atomic layer deposition (ALD).[6] However, these lanthanide oxide films had nanometer-thick interfacial layers when deposited on Si substrates, which made it impossible to scale the effective oxide thickness (EOT) to the subnanometer range. Previously, we found that interfacial layers could be avoided when ternary rare earth oxide ($GdScO_3$) films were deposited on Si by ALD from metal amidinate precursors and H_2O.[7] This research shows that ALD-deposited $LaScO_3$ and $LaLuO_3$ thin films have desirable structural and electrical properties, and are free of interfacial layers. Lanthanum yttrium oxide thin films were also deposited by ALD under the similar condition, in order to show the importance of the choice of the element combination.

Here we report ALD of $LaScO_3$ and $LaLuO_3$ thin films that are free of interfacial layers, while retaining the desirable high-κ and amorphous properties. Thus, we obtained films with EOT values <1 nm and very low leakage. Polycrystalline lanthanum yttrium oxide thin films were also deposited by ALD under similar conditions, showing the importance of the proper choice of element combinations.

Experimental

The oxide films were deposited in a flow-type ALD reactor with water vapor alternating with vapors of metal amidinate precursors: lanthanum tris(N,N'-di-*iso*-propylformamidinate), scandium tris(N,N'-diethylacetamidinate), lutetium tris(N,N'-diethylformamidinate), and yttrium tris(N,N'-di-*iso*-propylacetamidinate). The ternary oxide films $La_xM_{2-x}O_3$ (M = Sc, Lu, or Y) were deposited by repeatedly growing m-layers of La_2O_3 followed by n-layers of M_2O_3 with m, n = 1 or 2. The deposition temperature was 300°C for $LaScO_3$ and $LaLuO_3$, and 280°C for $La_xY_{2-x}O_3$. n-Type Si(100), with resistivity 0.5–1 Ω cm, was selected as the substrate. All substrates were treated in UV/ozone to remove surface organic contamination, then dipped into 10% aqueous HF solution for 5 s and rinsed with deionized water right before deposition. Metal-oxide-semiconductor (MOS) capacitors were made to measure the electrical properties. Tungsten nitride (WN) was deposited in the same ALD reactor as a top metal electrode.[8] Platinum dots were finally deposited by evaporation and liftoff and used as hard masks during the removal of exposed WN by reactive ion etching (CF_4 + Ar).

Results and Discussion

The film thickness and the number of ALD cycles have a linear relation with zero intercept (Fig. 1a), showing that growth begins immediately on H-terminated Si surfaces. For m, n = 1 or 2, the ternary oxide growth rate is approximately the summation of m times of the growth rate of La_2O_3 (1.3 Å/cycle) and n times of the growth rate of M_2O_3 (1.1 Å/cycle for Sc_2O_3, 1.2 Å/cycle for Lu_2O_3, and 0.8 Å/cycle for Y_2O_3). The impurity contents, including carbon and nitrogen, are below the detection limit (~1%) of X-ray photoelectron spectroscopy (XPS) (Fig. 1b). The film composition by Rutherford backscattering (not shown) depends on both the ratio m/n and the metal precursors. For $m = n = 1$, the ternary oxide films were determined to be $LaSc_{1.02\pm0.07}O_3$, $LaLu_{1.00\pm0.05}O_3$, and $La_{1.23}Y_{0.77}O_3$, respectively. The compositions of $La_xY_{2-x}O_3$ films for various m and n show a linear relationship between $x/2$ and $m/(m + 0.63n)$ with unit slope, which implies that the growth rate for each material is independent of the composition of the substrate that it is growing on. On the basis of this observation, $LaYO_3$ films can be obtained by setting $m = 2$ and $n = 3$.

Figure 2a shows a sharp interface between amorphous $LaScO_3$ and crystalline Si in a stack of $WN/LaScO_3/Si$. Similar results were found for $LaLuO_3$ and $La_xY_{2-x}O_3$ films [Cross-sectional transmission electron microscope (XTEM) images not shown]. The step coverage is close to 100% in holes with an aspect ratio of ~80:1. Figure 2b shows that a 12 nm $LaLuO_3$ film has a uniform thickness from the top to the bottom of the hole. Despite the fact that all the as-deposited binary oxides (M_2O_3) are polycrystalline body-centered-cubic phases determined by electron diffraction, both $LaScO_3$ and $LaLuO_3$ films are amorphous and homogeneous. In contrast, as-deposited $La_xY_{2-x}O_3$ films show a polycrystalline layer over an amorphous layer on Si by XTEM. The lattice incompatibility between these oxides and Si increases the activation energy barrier for nucleating crystalline phases adjacent to Si, resulting in an amorphous lower layer of $La_xY_{2-x}O_3$. After the growth of a thin amorphous layer (3–7 nm), the mismatch is relaxed so that a polycrystalline layer of $La_xY_{2-x}O_3$ can grow on the top.

MOS capacitors were made to measure the electrical properties. Figure 3a shows the high-frequency (1 MHz) capacitance-voltage (C-V) curves of $LaLuO_3$, $LaScO_3$, and $La_{1.23}Y_{0.77}O_3$ films with no

* Electrochemical Society Active Member.
z E-mail: gordon@chemistry.harvard.edu

Downloaded 29 Jan 2009 to 128.103.93.231. Redistribution subject to ECS license or copyright; see http://www.ecsdl.org/terms_use.jsp

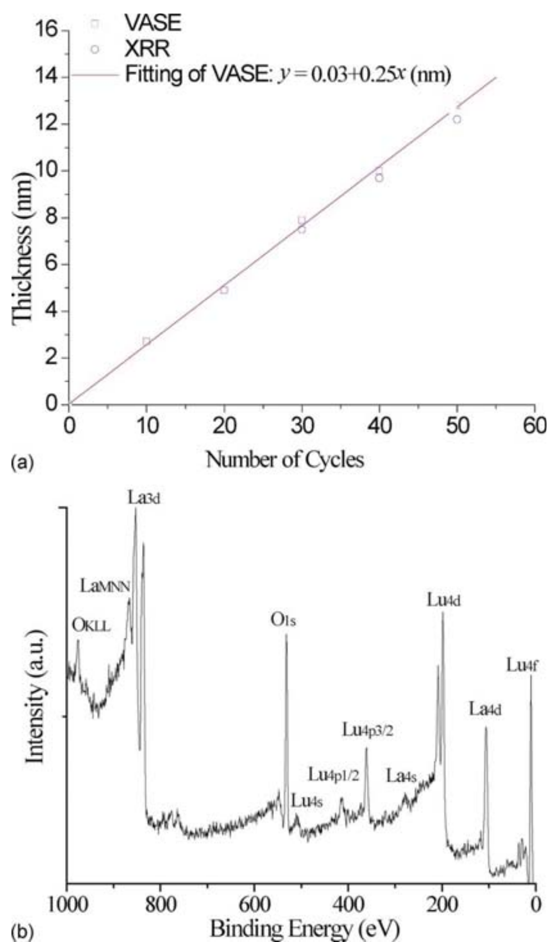

Figure 1. (Color online) (a) The thickness vs ALD cycle plot. The thickness was measured by both X-ray reflectivity (XRR) and variable angle scanning ellipsometer (VASE). (b) The XPS spectrum for $LaLuO_3$.

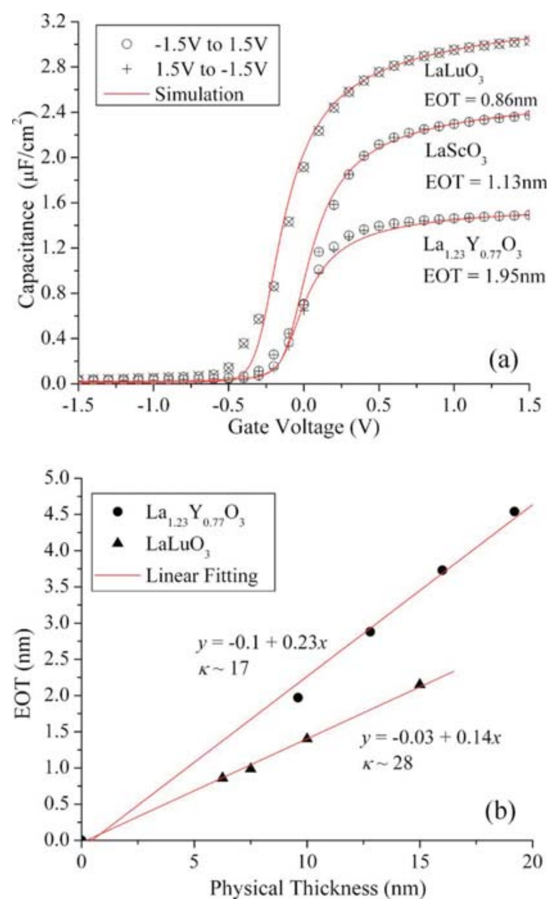

Figure 3. (Color online) (a) *C-V* curves measured at 1 MHz. The lines are simulated curves with MISFIT by assuming no interface traps. (b) The EOT plots as a function of the physical thickness.

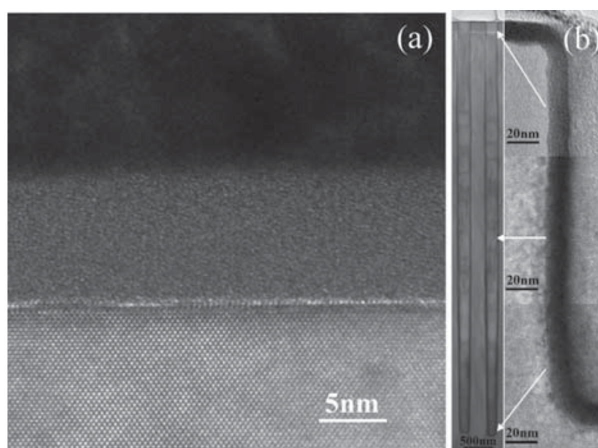

Figure 2. (a) XTEM image of a $WN/LaScO_3$ stack on Si substrate. The white line along the interface is caused by transmission electron microscope aberration. It consists of discrete spots, which are an extension of the Si lattice. (b) A 12 nm $LaLuO_3$ film deposited in holes with aspect ratio ~80:1. The hole has an elliptical cross section with semi-long axes 75 nm and semi-short axes 35 nm. Its depth is 7.2 μm. On the right-hand side are three higher magnification images for comparing the film thickness in the top, middle, and bottom parts of the trench.

noticeable stretching or shoulders. The small hysteresis (0–10 mV) indicates very few bulk traps in the films. The 10 and 100 kHz *C-V* curves (not shown) are closely aligned to 1 MHz ones with frequency dispersion less than 2–3% of the accumulation capacitance. Small shoulders appear in the weak inversion region of *C-V* curves measured at 10 and 100 kHz, which indicate the existence of some slowly responding interface states. The EOT was obtained by fitting the *C-V* data to ideal simulation curves using the Metal-Insulation-Semiconductor CV Fitting (MISFIT) program with charge quantization effect (Fig. 3a).[9] By linearly fitting the EOT vs physical thickness plot in Fig. 3b, the dielectric constants, extracted from the slopes, are 28 ± 1 and 17 ± 1.3 for $LaLuO_3$ and $La_{1.23}Y_{0.77}O_3$ films, respectively. The nearly zero intercept for $LaLuO_3$ films indicate the absence of any interfacial layer, consistent with the sharp interfaces observed by high-resolution XTEM. The dielectric constant for $LaScO_3$ is ~23, which is estimated by $\kappa = 3.9t_{physical}/EOT$. Both $LaScO_3$ and $LaLuO_3$ films have higher dielectric constants than those of their binary oxide components, i.e., La_2O_3 ($\kappa \sim 19$),[10] Lu_2O_3 (16), and Sc_2O_3 (17). These results imply that the amorphous ternary oxides form new microscopic structures, rather than simple mixtures of the two binary oxides. In view of the continuous random network theory,[11] it is possible that locally –O–La–O– (La^{3+} radius 103 pm) develops frames of polyhedrons with the smaller ions (Sc^{3+} radius 75 pm or Lu^{3+} 86 pm) caged inside. The Sc–O or Lu–O bonds are softened due to their smaller metal ion sizes, and the polarizability is therefore enhanced by the bond soft-

Downloaded 29 Jan 2009 to 128.103.93.231. Redistribution subject to ECS license or copyright; see http://www.ecsdl.org/terms_use.jsp

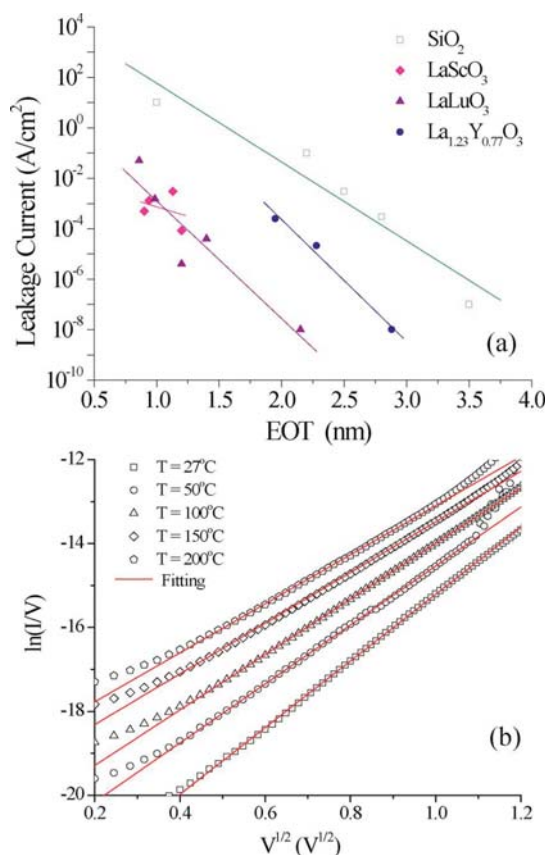

Figure 4. (Color online) (a) Leakage current density at $|V_g - V_{FB}| = 1$ V and (b) Poole–Frenkel plot of the leakage current density of a $LaScO_3$ film (EOT = 0.9 nm) at various temperatures.

ening, which can be more than enough to make up for an adverse effect caused by the relatively larger molar volume in the amorphous films.[12]

Figure 4a shows the leakage current density scaling of our ALD films compared to that of thermal SiO_2 films with the same EOT. The current density at 1 V gate bias ($|V_g - V_{FB}| = 1$ V) is up to 6 orders of magnitude lower than that of thermal SiO_2 for both $LaScO_3$ and $LaLuO_3$ films and 2–4 orders of magnitude lower for $La_{1.23}Y_{0.77}O_3$ films. All ternary oxide films have the same leakage current-voltage (J-V) behaviors. Figure 4b shows the J-V curves of a $LaScO_3$ film with 0.9 nm EOT at temperatures from room temperature to 200°C. The Poole–Frenkel plots (Fig. 3b) of this J-V measurement show linear behaviors in the range of 0.3–1.5 V. The dynamic refraction index calculated from the slopes is ~1.9 to 2.0, which is comparable to the optical refraction index measured at wavelength of 630 nm. The leakage currents also obey the Arrhenius law at different fixed voltages (not shown). Combining these two observations, we conclude that $J = cV \exp\{-[(\phi_B - \beta_{PF}V^{1/2})/k_BT]\}$, which is exactly the Poole–Frenkel formula. The extracted trap depth ϕ_B is 0.3–0.4 eV.

Conclusions

In summary, $La_xM_{2-x}O_3$ (M = Sc, Lu, or Y) films were deposited by ALD with metal amidinate precursors and H_2O. Both $LaScO_3$ and $LaLuO_3$ films are amorphous and free of interfacial layers. Besides the structural benefits, both oxides have high dielectric constants (~23 for $LaScO_3$ and 28 ± 1 for $LaLuO_3$), low leakage current density, and very few bulk traps, and are scalable to EOT < 1 nm. $La_{1.23}Y_{0.77}O_3$ films have polycrystalline structures with moderately high $\kappa = 17 \pm 1.3$ and low leakage current. The Poole–Frenkel mechanism is verified in the ternary oxide films by studying temperature dependence of the leakage current.

Acknowledgments

This work was supported in part by Rohm and Haas Electronic Materials and performed, in part, at Harvard University's Center for Nanoscale Systems, a member of the National Nanotechnology Infrastructure Network, supported by the U.S. National Science Foundation under award no. ECS-0335765. We also thank Professor Ramanathan for helping in the leakage current measurement.

Harvard University assisted in meeting the publication costs of this article.

References

1. http://www.intel.com/technology/architecture-silicon/45nm-core2/
2. H. Kim, P. C. McIntyre, and K. C. Saraswat, *Appl. Phys. Lett.*, **82**, 106 (2003).
3. J. Robertson, *Mater. Res. Bull.*, **27**, 217 (2002).
4. J. M. J. Lopes, U. Littmark, M. Roeckerath, St. Lenk, J. Schubert, and S. Mantl, *J. Appl. Phys.*, **101**, 104109 (2007); J. M. J. Lopes, M. Roeckerath, T. Heeg, U. Littmark, J. Schubert, S. Mantl, Y. Jia, and D. G. Schlom, *Microelectron. Eng.*, **84**, 1890 (2007).
5. J. M. J. Lopes, M. Roeckerath, T. Heeg, E. Rije, J. Schubert, S. Mantl, V. V. Afanas'ev, S. Shamuilia, A. Stesmans, Y. Jia, et al., *Appl. Phys. Lett.*, **89**, 222902 (2006).
6. J. H. J. Lopes, M. Roeckerath, T. Heeg, J. Schubert, U. Litmark, S. Mantl, A. Besmehn, P. Myllymaki, L. Niinisto, C. Adamo, et al., *ECS Trans.*, **11**(4), 311 (2007).
7. K. H. Kim, D. B. Farmer, J.-S. M. Lehn, P. V. Rao, and R. G. Gordon, *Appl. Phys. Lett.*, **89**, 133512 (2006).
8. J. S. Becker, S. Suh, S. Wang, and R. G. Gordon, *Chem. Mater.*, **15**, 2969 (2003).
9. G. Apostolopoulos, G. Vellianitis, A. Dimoulas, J. C. Hooker, and T. Conrad, *Appl. Phys. Lett.*, **84**, 260 (2004).
10. H. Yamada, T. Shimizu, A. Kurokawa, K. Ishii, and E. Suzuki, *J. Electrochem. Soc.*, **150**, G429 (2003); S. Y. No, D. Eom, C. S. Hwang, and H. J. Kim, *J. Appl. Phys.* **100**, 024111 (2006); W. M. He, S. Schuetz, R. Solanki, J. Belot, and J. McAndrew, *Electrochem. Solid-State Lett.*, **7**, G131 (2004).
11. R. Zallen, *The Physics of Amorphous Solids*, Wiley-VCH, Hoboken, NJ (1998).
12. E. Cockayne, *J. Appl. Phys.*, **103**, 084103 (2008).

Downloaded 29 Jan 2009 to 128.103.93.231. Redistribution subject to ECS license or copyright; see http://www.ecsdl.org/terms_use.jsp